

Methodological considerations for studying spectral-plant diversity relationships

Christine I.B. Wallis^{a,*}, Anna L. Crofts^b, Robert Jackisch^a, Shan Kothari^{c,d}, Guillaume Tougas^{b,c}, J. Pablo Arroyo-Mora^e, Paul Hacker^f, Nicholas Coops^f, Margaret Kalacska^g, Etienne Laliberté^c, Mark Vellend^b

^a Geoinformation in Environmental Planning Lab, Technical University of Berlin, 10623 Berlin, Germany

^b Département de Biologie, Université de Sherbrooke, Sherbrooke J1K2R1, Québec, Canada

^c Département de Sciences Biologiques et Université de Montréal, Institut de Recherche en Biologie Végétale, Montréal H1X 2B2, Québec, Canada

^d Faculty of Agricultural, Life and Environmental Sciences, Department of Renewable Resources, University of Alberta, Alberta T6G 2G7, Canada

^e Flight Research Laboratory, National Research Council of Canada, Ottawa, Ontario K1A 0R6, Canada

^f Integrated Remote Sensing Studio, Department of Forest Resources Management, University of British Columbia, Vancouver V6T 1Z4, British Columbia, Canada

^g Applied Remote Sensing Lab, Department of Geography, McGill University, Montréal H3A 0B9, Quebec, Canada

ARTICLE INFO

Editor: Dr. Marie Weiss

Keywords:

Hyperspectral
A-Diversity
Plant diversity
Spectral diversity
Illumination corrections
Functional plant diversity
Shadow
Spatial resolution

ABSTRACT

The Spectral Variation Hypothesis (SVH) posits that higher spectral diversity indicates higher biodiversity, which would allow imaging spectroscopy to be used in biodiversity assessment and monitoring. However, its applicability varies due to ecological and methodological factors. Key methodological factors impacting spectral diversity metrics include spatial resolution, shadow removal, and spectral transformations. This study investigates how these methodological considerations affect the application of the SVH across ecosystems and sites. Using field and hyperspectral data from forest and open (e.g., wetland, grassland, savannah) ecosystems from five sites of the Canadian Airborne Biodiversity Observatory (CABO), we analyzed three variance-based spectral diversity metrics across and within vegetation sites, examining the effects of illumination corrections, spatial resolution, and shadow filtering on the spectral-plant functional diversity relationship. Our findings highlight that the relationship between spectral diversity metrics and functional diversity are strongly influenced by methods, especially spectral transformations. These illumination corrections notably impacted the spectral regions of importance and the resulting relationships to plant functional diversity. Depending on methodological choices, we observed correlations that varied not only in strength but also direction: in open vegetation we saw negative correlations when using brightness normalization, and positive correlations when using continuum removal. Shadow removal and spatial resolution were important but had less impact on the correlations. By systematically analyzing these methodological aspects, our study not only aims to guide researchers through potential challenges in SVH studies but also highlights the inherent sensitivity of spectral-functional diversity relationships to methodological choices. The variability and context-dependence of these relationships across and within sites emphasize the need for adaptable, site-specific approaches, presenting a key challenge in developing robust methods to enhance biodiversity monitoring and conservation strategies.

1. Introduction

Remote sensing has emerged as an essential tool for vegetation assessment monitoring across landscapes, extending its potential beyond traditional field inventories (Coops et al., 2023; Goetz and Dubayah, 2011; White et al., 2016). A key technique in ecological remote sensing is reflectance spectroscopy, which involves the

measurement of electromagnetic radiation reflected by Earth's surfaces between ~350–2500 nm (the reflectance spectrum). Reflectance products from image spectroscopy enables the detection of nuanced information related to plant health, composition, and structural attributes within ecosystems (Cavender-Bares et al., 2017; Huete, 2004; Wang and Gamon, 2019). By incorporating wavelengths beyond the visible spectrum (> 700 nm), it enhances the ability to quantify and analyze

* Corresponding author.

E-mail address: christine.wallis@tu-berlin.de (C.I.B. Wallis).

ecological traits such as vegetation structure and overall plant state (Jacquemoud and Ustin, 2019).

The concept of spectral diversity—the variation in reflectance spectra within a specific area—is central to the Spectral Variation Hypothesis (SVH). This hypothesis posits that greater spectral diversity within a given area reflects greater biodiversity and functional complexity (Palmer et al., 2002). Although the SVH offers a straightforward premise, studies present divergent findings, suggesting that it may be challenging to implement the SVH in a way that applies universally (Fassnacht et al., 2022; Thornley et al., 2023). This concern restricts its potential use for biodiversity mapping or monitoring via remote sensing.

To understand the applicability of the SVH, many studies have explored various ecological factors to determine when it is successful. For example, the strength of relationships in SVH models tends to be higher in vegetation with a higher leaf area index (Schweiger and Laliberté, 2022), simpler vertical canopy structures (Conti et al., 2021), less biomass variability (Rossi et al., 2022), and more pronounced environmental gradients (Wallis et al., 2024). Phenological factors also play a crucial role with contrasting phenological patterns of spectral diversity metrics emerging at leaf and canopy scales (Wang et al., 2022). Additionally, functional plant diversity often shows stronger correlations with spectral diversity compared to taxonomic diversity (Crofts et al., 2024a; Wallis et al., 2024). These factors influence the results and conclusions drawn from the SVH by affecting how ecological processes interact and manifest in different settings. However, it is challenging to compare the findings of these studies due to methodological differences, whose impacts have yet to be explored systematically.

A major difference among studies addressing the SVH is their spatial resolution. While some studies utilize data of medium to coarse spatial resolution from 10 to 500 m per pixel (Lopes et al., 2017; Schmidlein and Fassnacht, 2017), findings like those from Lopatin et al. (2017) advocate aligning the sensor's spatial resolution with the scale of individual plants. In grassland environments, for instance, spatial resolutions are often on the centimeter scale, sometimes finer than 1 cm in order to avoid the capture of reflectance from multiple species within a single pixel (Hacker et al., 2022). Therefore, a high spatial resolution (1 cm - 2 m depending on the target species) is crucial for accurately capturing the spectral signatures of individual plants. At these finer resolutions, however, challenges arise, particularly the effects of canopy shadows. Canopy shadows, which result from varying light conditions under the canopy, can distort spectral data (Zhang et al., 2015). Mixed pixels, which contain signals from both vegetated and shadowed or non-vegetated areas, complicate the spectral reflectance data and obscure the true spectral signatures of the target species. Although some studies have examined the impact of spatial resolution on vegetation monitoring (Lopatin et al., 2019; Milas et al., 2017; Zhang et al., 2015), fewer studies have also considered canopy and cloud shadow effects.

The potential for addressing shadow effects varies across ecosystems and depends on data availability. In forest ecosystems, shadow removal is relatively straightforward; simulated shaded pixels at the time of acquisition can be created from a canopy surface model derived from photogrammetry or light detection and ranging (LiDAR) data (Grubinger et al., 2023). However, such data and techniques are not always available or feasible in other habitats when individual plants are much smaller, as in grasslands. Consequently, most studies continue to rely on thresholding reflectance data to remove dark pixels classified as shadows (Adeline et al., 2013; Badourdine et al., 2023; Lopatin et al., 2019; Rüfenacht et al., 2014; Schweiger and Laliberté, 2022). To address these differences and evaluate the generality of methodological outcomes, we included both forest and open vegetation sites in our analysis. This allowed us to assess spectral-plant diversity relationships across contrasting functional types and spatial resolutions, providing a more robust evaluation of how methodological choices scale across ecosystems.

In airborne hyperspectral data, fine spatial resolution often

highlights what we can consider non-ecological variation, which arises from factors such as heterogeneous illumination conditions between and within flight lines, unrelated to vegetation properties, and leading to a significant increase in spectral variation that is unrelated to the reflectance properties of plant tissues (Arroyo-Mora et al., 2021; Behmann et al., 2016; Manea and Calin, 2015). In contrast, 'ecological variations' refer to variability in the data that is due to actual ecological processes, such as differences in vegetation structure, species composition, or phenological stages. However, separating illumination effects from ecologically meaningful spectral variation is challenging. Illumination conditions are influenced not only by sensor and solar and sensor geometry but also by real ecological differences, such as canopy structure, vegetation height, or slope orientation. Thus, standard correction methods risk either leaving residual artifacts or inadvertently removing important biological signals. Recognizing this conundrum, several correction techniques have been developed to address illumination-related variation, such as the spectral angle mapper, brightness normalization, and continuum removal (Clark and Roush, 1984; Feilhauer et al., 2010; Féret and Asner, 2014; Jänicke et al., 2020; Kruse et al., 1993). While we recognize the existence of a wide range of hyperspectral image processing methods in foundational remote sensing literature (e.g., Eismann, 2012), this study focuses on a subset of approaches more widely employed in the ecological context. For instance, to account for varying light conditions, brightness normalization adjusts all pixels to a vector magnitude of 1 (Feilhauer et al., 2010). Continuum removal emphasizes specific absorption features by removing the general spectral background, which might also reduce effects from varying illumination conditions (Clark and Roush, 1984; Serbin and Townsend, 2020). While these spectral transformations are crucial for reducing brightness variations and enhancing the comparability of spectral reflectance data from high-resolution imagery, they may also lead to the loss of information related to variations in canopy structure. Overall, the effects of these two spectral transformations have been rarely compared in spectral diversity studies (Badourdine et al., 2023; Imran et al., 2021).

Once these corrections are applied, spectral diversity indices can be calculated from the data (Chang, 2000; Dahlin, 2016; Frye et al., 2021; Gholizadeh et al., 2018). The sensitivity of spectral diversity to non-ecological variation depends on the sensitivity of the metrics to outliers. Common indices employed to capture spectral variation include the squared mean distance of spectral values to the spectral centroid (Laliberté et al., 2020), the coefficient of variation (Gholizadeh et al., 2018), and ordination-based metrics such as convex hull volume (Gholizadeh et al., 2018). These metrics, which are analogous to metrics of plant functional diversity, vary in their sensitivity to outliers. Spectral diversity metrics can be calculated based on the full spectrum or selected wavelength bands which poses another source of variation in SVH studies. Some studies claim that the choice of bands is of high importance (Gholizadeh et al., 2018; Wang et al., 2018), though the optimal spectral region for calculating spectral diversity can also depend on the investigated vegetation type (Wallis et al., 2024). Therefore, the choice of spectral diversity metrics and incorporated wavelength bands might have important consequences for assessments of plant diversity.

Methodological aspects - particularly the combined effects of spatial resolution, shadow removal, and spectral transformations - require systematic analysis to understand their influence on the success of the SVH. Here we explore the effects of key methodological decisions on variance-based spectral diversity metrics and their relationships to plant functional diversity. Using field and hyperspectral data covering visible (VIS) to near infrared (NIR) wavelengths in forest and open ecosystems within Canada, we examine the impact of spatial resolution, shadow removal, and spectral transformations (brightness normalization vs. continuum removal). We quantified correlations between plant functional diversity and different variance-based spectral diversity metrics, and tested how these correlations and the importance of different wavelength bands between 450 and 900 nm depend on methodological decisions. Our focus is on guiding researchers through potential

challenges and pitfalls in SVH studies at the landscape scale.

2. Data and methods

2.1. Study sites

The Canadian Airborne Biodiversity Observatory (CABO) is an initiative that utilizes airborne remote sensing technologies to monitor and study biodiversity across Canada. It consists of a network of diverse sites selected to capture a broad range of ecosystem types (wetland, temperate forest, boreal forest, grassland, savannah), while also being accessible and well-studied.

To test the SVH in open vegetation and forests, we used five out of six sites from the CABO project located in southern Quebec, Ontario and coastal British Columbia (Fig. 1, Table 1). Open vegetation includes the grassland portion of a savannah (Cowichan Garry Oak Preserve, CGOP; surveyed in May 2019, see also (Hacker et al., 2022), a peatland (Mer Bleue, MB; surveyed in July 2019, (Girard et al., 2020), and an abandoned agricultural field within Parc national des îles-de-Boucherville (Île Grosbois de Boucherville, IGB; surveyed in August 2018, Elmer et al., 2021). The two forest sites are located within Parc national du Mont-Saint-Bruno (MSB) and Parc national du Mont-Mégantic (MMG), both in Québec, surveyed in 2018, 2019 and 2020 (Crofts et al., 2024a; Wallis et al., 2023). Unfortunately, another CABO site in the Arctic could not be included because field data sampling and UAV flights were postponed due to the pandemic in 2020.

2.2. Vegetation surveys

Plant inventories were conducted in 2018, 2019 and 2020. Open vegetation plots were $3\text{ m} \times 3\text{ m}$ quadrats, and forest plots were circular with a radius of 15 m. All plant inventories followed standardized protocols from the CABO project (Crofts et al., 2022; St-Jean and Vellend, 2020). Because we expect the spectral diversity-plant diversity

relationship to be strongest when only the plant portions exposed to direct overhead light are used, we measured species abundance from the canopy as visible from above. For open vegetation, field inventories to quantify species abundance were done visually from an elevated ladder in the field or using images from small drones where applicable (St-Jean and Laliberté, 2020). For forests, all crowns were delineated in the field and we applied a GIS-based approach to extract the top crown layer using the ‘sf’ package in R (Pebesma, 2018; for details see Wallis et al., 2023).

Leaf trait measurements at the five sites followed the CABO trait sampling protocols (Ayotte and Laliberté, 2019; Laliberté, 2018). We selected three traits with high coverage across species at our sites: leaf nitrogen concentration (N; mass-based), leaf dry matter content (LDMC) and leaf mass per area (LMA). To enhance trait coverage up to more than 99 % per plot, we used a gap-filling procedure to fill in missing trait values for certain species with trait values from the TRY database (Kattge et al., 2020; see supplementary data in Wallis et al., 2024). We note that the use of imputed trait values from the TRY database may introduce additional uncertainty. However, because the majority of trait data were collected directly in the field and only a small proportion of values were gap-filled, we expect the overall impact on trait variation and downstream analyses to be minimal. We calculated functional diversity using the ‘FD’ package in R (Laliberté et al., 2014; Laliberté and Legendre, 2010). Specifically, we used functional dispersion (FDis), which was weighted by species abundance. FDis considers the dispersion of species in trait space relative to the centroid and can accommodate communities with a single plant species.

2.3. Hyperspectral surveys

Hyperspectral surveys were conducted alongside the plant inventories in 2018, 2019 and 2020 using two comparable hyperspectral pushbroom imagers that collected spectral information across 288 spectral bands covering the visible and near-infrared (NIR) regions

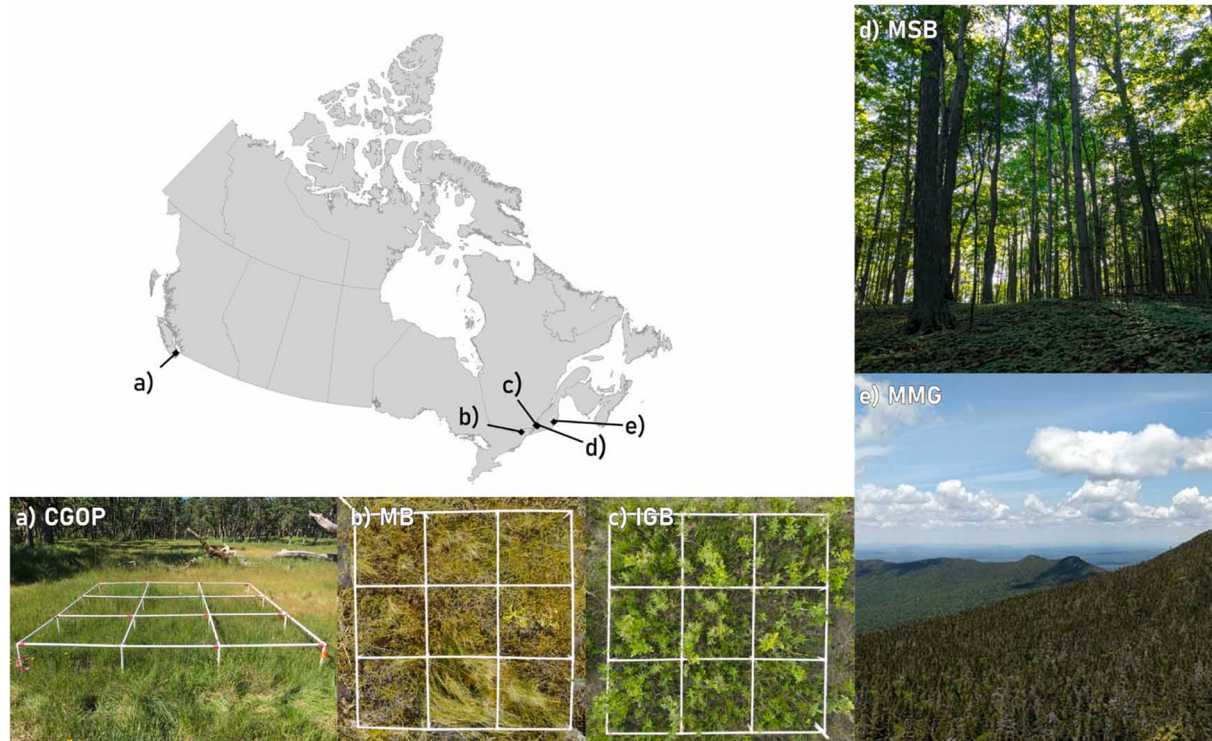


Fig. 1. Study sites located across Canada are a) a grassland (CGOP), b) a peatland (MB), c) an abandoned agricultural site (IGB) as well as two forested sites (d) MSB and e) MMG. MMG is characterized by a transition from deciduous to coniferous species along with higher elevation. Figure adapted from Wallis et al. (2024). photographs from the five sites.

Table 1
A summary of all projects with details on the samples and the timing of field and airborne surveys included in the study. Viewing geometry (off-nadir viewing angle) refers to pixel-level angles of the investigated plots per site (see also supplementary fig. S2).

Site	Description	Field site and investigated plots			Field survey		Airborne survey			
		Latitude	Longitude	No. of plots	Species richness	Plant survey and plot design	Airborne survey and sensor used	Flight time (GMT)	Local time	Flight Altitude (m)
Cowichan Garry Oak Preserve, CGOP	Savanna/ grassland in British Columbia Peatland	48° 48.5' N 45° 24' N	123° 37.8' W −75° 30' W	21 8	55 21	May 2019, Squares, 4 m × 4 m (16 m ²) July 2019, Squares, 4 m × 4 m (16 m ²)	May 2019, µCASI µCASI	18:30–20:40 14:54–18:25	11:30–13:40 10:54–14:25	60 m 45 m
Île Grosbois de Boucherville, IGB	Abandoned agricultural field within Parc national des îles-de-Boucherville Environmentally less diverse and warmer than MMG, with more southerly species.	45° 37.6' N	73° 28' W	25	30	August 2018, Squares, 4 m × 4 m (16 m ²) 2019–2020, Circular, radius of 15 m (707 m ²)	August 2018, µCASI September 2018, CASI-1500	11:53–16:33 14:59 (single flight line)	7:53–12:33 10:59	45 m 1680 m
Parc national du Mont-Saint-Bruno, MSB	Spans an elevation gradient from deciduous temperate forest to coniferous boreal forest	45° 27' N	−71° 10' W	49	23	2019–2020, Circular, radius of 15 m (707 m ²)	July 2019, CASI-1500	14:35–15:28	10:35–11:28	1680 m
Parc national du Mont-Mégantic, MMG										10:82° (5.22°)

(Table 1). The µCASI sensor used at the open vegetation sites was mounted on an unoccupied aerial vehicle (UAV) and recorded data resampled to a pixel size of 3 cm (401–995 nm; Arroyo-Mora et al., 2019). The CASI-1500 sensor used at forest sites was onboard the Twin Otter fixed-wing aircraft operated by the National Research Council of Canada, Flight Research Lab (NRC-FRL) and recorded data resampled to ~2 m pixel size (375–1061 nm; Inamdar et al., 2021a). The spectral resolutions of the two sensors were comparable, with µCASI offering a full width at half maximum (FWHM) of approximately 2.1 nm, and the CASI-1500 a slightly broader FWHM of around 2.4 nm. To ensure spectral consistency across sensors, all µCASI data were spectrally resampled to match the spectral response of the CASI-1500 prior to further analyses (see next section *hyperspectral post-processing*). Given the high spectral resolution of both sensors and the resampling step, differences in spectral resolution are unlikely to have influenced the subsequent analyses.

Most hyperspectral flights were conducted around solar noon, when the solar zenith angle was lowest and the solar elevation angle approached its daily maximum (typically around 60–70° at our sites), meaning that illumination conditions were optimal and shadowing effects were minimal. The one exception was Îles-de-Boucherville (Table 1) where the park required that the UAV flights be completed early morning to minimize disruption to the park visitors. The raw hyperspectral data underwent standard pre-processing steps, including a radiometric, and atmospheric correction (Inamdar et al., 2021b). The atmospheric correction was applied in ATCOR-4 software, which utilizes a Look-Up Table (LUT) method for atmospheric correction following the approach in Soffer et al. (2019). This approach is consistent with the methods employed in Arroyo-Mora et al. (2021) and Inamdar et al. (2021a, 2021b), who utilized the same data and processing techniques as in our study (see also Fig. S1).

For the MMG imagery, a topographic correction was applied due to its elevation gradient, which spans from deciduous temperate forest to coniferous boreal forest. The presence of varying slopes and surface types in this area necessitated a correction to account for incident angle effects on the spectral reflectance. This correction was implemented using the Lambert + Statistical-Empirical approach (Richter and Schläpfer, 2019), and used LiDAR data from the Ministry of Forests, Wildlife, and Parks of Québec (Leboeuf and Pomerleau, 2015). The LiDAR dataset was provided as a 1 m pixel size Digital Surface Model (DSM). Other sites in this study did not require a topographic correction as they exhibited relatively flat terrain, where such effects were less significant. Airborne imaging spectroscopy and field survey data for the forested sites is publicly available (Crofts et al., 2024b).

While airborne CASI-1500 flights were also conducted over some of the non-forested sites (IGB and MB), µCASI UAV flights were not conducted over forests. We decided not to use CASI-1500 data for open vegetation sites due to the discrepancy between the species' individual size and the pixel size of the airborne imagery.

2.4. Hyperspectral data extraction and preprocessing

We extracted the hyperspectral data for each field plot, using spectral data with a lower off-nadir viewing angle when plots were covered by overlapping flight lines (see fig. S2). We then applied spatial resampling, post-processing steps, shadow masking, illumination corrections, and calculated spectral diversity metrics, as detailed below.

2.5. Spatial resampling

We resampled all hyperspectral images of open vegetation to a pixel size of 3 cm, 10 cm, 30 cm and 60 cm using averaging following the approach in Wang et al. (2018). For this purpose, we used a pixel-wise approach in the stars package in R (Pebesma and Bivand, 2023); we however did not consider the point spread function which is described in Inamdar et al. (2023). We also did not resample the images from forested

sites since we considered the spatial resolution of approximately 2 m already broad.

2.6. Hyperspectral post-processing

Post-processing included removing non-vegetated pixels using NDVI thresholds (open vegetation: NDVI < 0.35; forests: NDVI < 0.75), masking spectral regions with low signal quality (< 450 nm) and strong residual atmospheric water absorption (> 900 nm), spectral resampling of μCASI using the spectral response functions of CASI-1500 data in the hsdar package in R (Lehnert et al., 2019) to enhance comparability between the two sensors, and spectral smoothing using a Savitzky-Golay filter with a defined window size of 21 bands and a polynomial of 4th order.

2.7. Shadow masking

Many UAV studies have performed shadow masking based on visual interpretation of shadowed pixels and reflectance-based histogram thresholding (e.g. Lopatin et al., 2019). However, visual interpretation of shadowed pixels is highly subjective, and different thresholds can be set from very conservative to minimal shadow influence. We therefore removed shadowed pixels by using thresholds in a red band (679 nm) for forests and a red-edge band (720 nm) for open vegetation. We applied multiple thresholds for shadow removal in both open vegetation and forest sites to assess how varying threshold levels affect the results. Specifically, thresholds were tested at low, medium, and high levels (Fig. S3) to evaluate their sensitivity and impact on shadow filtering. Plots with more than 60 % of pixels identified as shadow were excluded from the analyses to ensure consistency and accuracy in our data.

2.8. Illumination corrections

To reduce the impact of brightness differences across all sites and plots, we applied two spectral processing techniques: brightness normalization and continuum removal. Brightness normalization, following the approach of Feilhauer et al. (2010), adjusts each pixel's spectral values by dividing the entire spectral vector by its magnitude. This process minimizes variation due to differences in illumination. Continuum removal is a method used to highlight absorption features in spectral data by removing the influence of broad spectral trends. It involves dividing or subtracting the reflectance values by a continuum line that fits the spectral shape, thus emphasizing smaller absorption features. We employed a segment hull approach for continuum removal, which detects these features more precisely. Specifically, we calculated the band depth by dividing the reflectance by the segment hull as well as the difference by subtracting the reflectance from the segment hull, as described by Obermeier et al. (2019) and Lehnert et al. (2019):

$$BD_w = 1 - (\text{REF}_w / \text{SH}_w)$$

and

$$\text{DIFF}_w = \text{SH}_w - \text{REF}_w,$$

where SH is the continuum value from the segment hull at wavelength band w.

The results of the illumination corrections were visualized for subsets of flight lines for MB and MSB (see fig. S4). After continuum removal, the start and end bands had to be removed, and 187 spectral bands remained which we used to calculate spectral diversity. For comparability, we removed the same bands in brightness normalized spectra.

2.9. Calculation of spectral diversity

For all combinations of shadow filtering, pixel sizes, and illumination correction methods, we calculated three variance-based spectral di-

versity metrics: The mean absolute deviation (Wallis et al., 2024), the squared distance to the centroid (Sdiv, Laliberté et al., 2020) and the coefficient of variation (CV; Wang et al., 2018). While there are other spectral diversity metrics, we chose these ones because they are used most often in literature. They are calculated as follows:

$$\text{MAD} = (1/n) \sum |x_i - \mu|$$

where n represents the number of spectral bands, x_i denotes the value of each individual band i and μ is the mean of all spectral measurements.

$$\text{Sdiv} = \sum (x_i - \mu)^2$$

where x_i denotes the value of each individual band i and μ is the mean of all spectral measurements.

$$\text{CV} = (\sigma/\mu) \times 100$$

where σ is the standard deviation of the spectral measurements and μ is the mean of the spectral measurements.

To account for the removal of shadowed pixels and varying numbers of pixels per plot, we used a bootstrap procedure with 30 iterations, randomly sampling the minimum available number of pixels per plot for each shadow and pixel size combination.

2.10. Statistical approach

To systematically assess how different methodological settings affect the relationship between spectral diversity and plant functional diversity, we first calculated Pearson correlation coefficients across various combinations of pixel sizes, spectral diversity metrics, shadow filtering thresholds, and illumination correction methods. In addition, we tested Spearman's rank and Kendall's tau correlation coefficients to provide non-parametric comparisons (see Supplementary Information for detailed results). Analyses were conducted separately for open vegetation and forest sites, using the same set of field plots (44 open vegetation plots and 49 forest plots) to ensure consistency and comparability.

To further explore variation in these relationships across spatial scales and among sites, we calculated correlations across all sites and within individual sites. For this analysis, we applied a mid-level shadow filter and used a pixel size of 3 cm for the open ecosystems, incorporating all available plots for this combination, resulting in 54 plots for open vegetation and 60 plots for forests.

Finally, to identify the most informative spectral regions for detecting functional diversity, we analyzed correlations between spectral diversity and plant functional diversity at individual wavelength bands using Pearson, Spearman's rank, and Kendall's tau coefficients. This band-specific analysis also employed the mid-level shadow filter and 3 cm pixel size and was conducted separately for each spectral transformation method.

3. Results

The functional composition of vegetation across the study sites was assessed using community-weighted means (CWMs) of leaf dry matter content (LDMC), leaf mass per area (LMA), and nitrogen concentration (N; mass-based) (Fig. 2). The resulting trait space captures broad site-level differences indicating diverse environmental gradients of the sites. Forested sites were distributed along an elevational gradient, with higher LDMC and LMA values corresponding to higher elevations. Open sites exhibited greater variation in nitrogen concentration indicative of differing nutritional regimes. The peatland site, Mer Bleue, showed elevated LMA values relative to other open-canopy sites reflecting a greater prevalence of shrubs compared to other open areas.

Our analysis revealed significant spectral variation across and within the analyzed vegetation sites, particularly in the NIR range (Fig. 3). Open vegetation sites exhibited a notably higher range of spectral

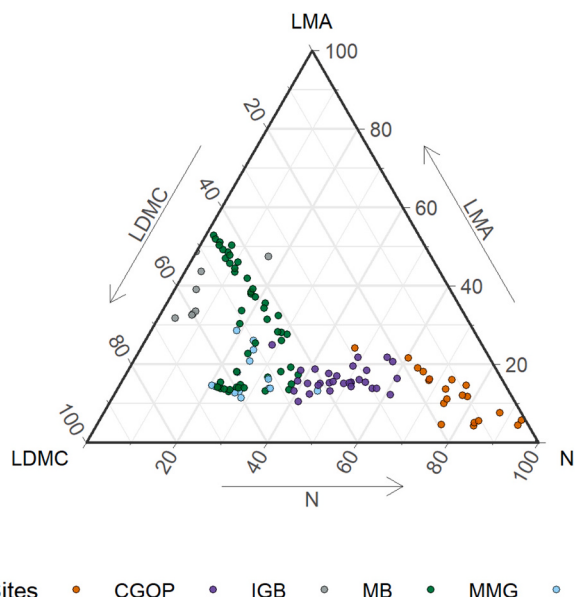


Fig. 2. Ternary plot of community-weighted mean (CWM) trait composition per plot across all studied CABO sites. Points represent plots, positioned according to the proportion of three standardized traits: leaf nitrogen concentration (N), leaf mass per area (LMA), and leaf dry matter content (LDMC). Trait values were min-max scaled across all plots and normalized so their proportions sum to 1 per plot. Colors indicate sites. Data reflect differences in dominant trait strategies among ecosystems.

reflectance values (Fig. 3 a), which can be attributed to both the intrinsic ecological differences (such as vegetation structure and species combination) and non-ecological factors, including sensor-related noise, variation in illumination conditions, bare soil exposure, and other background effects. Specifically, the prairie site (CGOP) displayed a distinct spectral shape from other sites. This difference was consistent across all applied processing methods and calculated metrics (Fig. 4). However, the spectral regions with peaks of spectral variation differed notably across open vegetation sites when using brightness normalization compared to continuum removal.

3.1. Impact of spectral processing methods and spectral diversity metrics on spectral patterns

In examining the impact of different spectral processing methods, we found that brightness normalization maintains the characteristic shape of vegetation spectra (Fig. 4 a and d). In contrast, both continuum

removal approaches altered the spectral shape by minimizing overall brightness and emphasizing specific absorption features in the visible range (Fig. 4 b–c, e–f). Band depth enhanced relative absorption strengths, while the difference produced spectra centered around zero by subtracting the continuum hull from the original reflectance. Both continuum removal approaches reduced values in the NIR region and amplified variation in the VIS range, altering the relative relationships between bands.

The calculation of spectral diversity metrics indicated that MAD and Sdiv are very similar in their outcomes (Fig. 4, second and third row), even though Sdiv might be more prone to outliers. The peaks of MAD, Sdiv and CV, however, differed depending on the choice of the illumination correction, and the type of vegetation. For instance, in open vegetation MAD derived from brightness normalization showed different peaks in spectral variation for the three sites (Fig. 4 g) while MAD based on both continuum-removed spectra showed two more uniform peaks around 450 nm and 650 nm for all the open vegetation sites (Fig. 4 h–l, k–l).

Our results also indicated that the CV calculated from continuum removal might not provide reliable information in this context (Fig. 4 t–u, w–x), as this method emphasizes wavelengths with low band depth values, which are disproportionately near zero following division or subtraction by the segment hull. This observation indicates that such values do not accurately reflect low raw reflectance values, so that standardization by the mean might not be meaningful.

3.2. Methodological effects on spectral-plant diversity relationships

The relationship between spectral and plant functional diversity was markedly dependent on the illumination correction method and the spectral diversity metric (Fig. 5). In open vegetation, we found negative relationships when calculating spectral diversity based on brightness-normalized spectra as well as weak to negative relationships for continuum removal based on subtraction (CR – difference; Fig. 5). In contrast, forested areas showed universally positive relationships across all metrics and methods, but certain combinations showed stronger relationships, such as those involving MAD. These patterns were consistent when using non-parametric correlation coefficients, including Kendall's tau and Spearman's rho (Fig. S5, S6). Pixel size and shadow filtering also influenced the spectral-plant diversity relationship, but their influence was weaker than the processing methods and metrics. In open vegetation, most relationships were weaker when using reflectance data at 60 cm pixel size. No relationship was observed for the CV based on continuum-removed spectra at a pixel size of 10 cm, contrasting with the findings at other pixel sizes for this combination. At forest sites, shadow filtering generally strengthened relationships, although the threshold levels did not always need to be high.

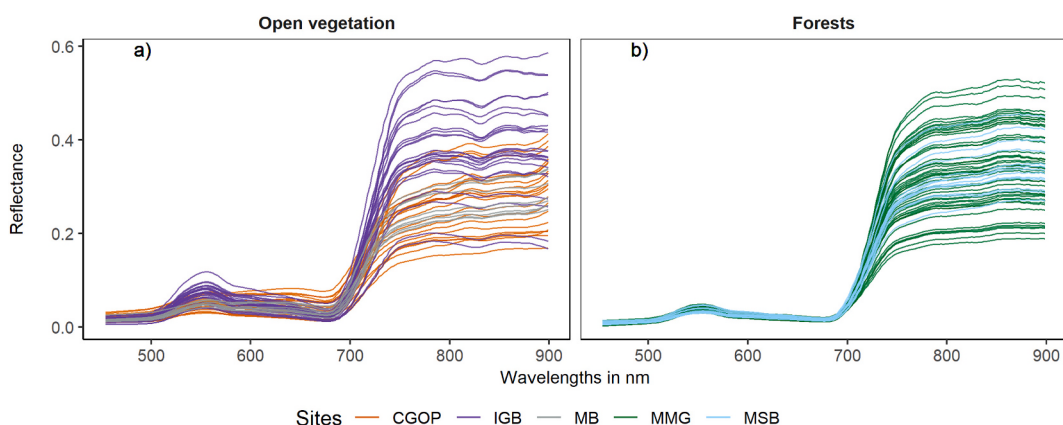


Fig. 3. Plot-wise averaged spectral reflectance for open vegetation and forests using the smoothed mean reflectance values for each plot. Colors indicate different sites.

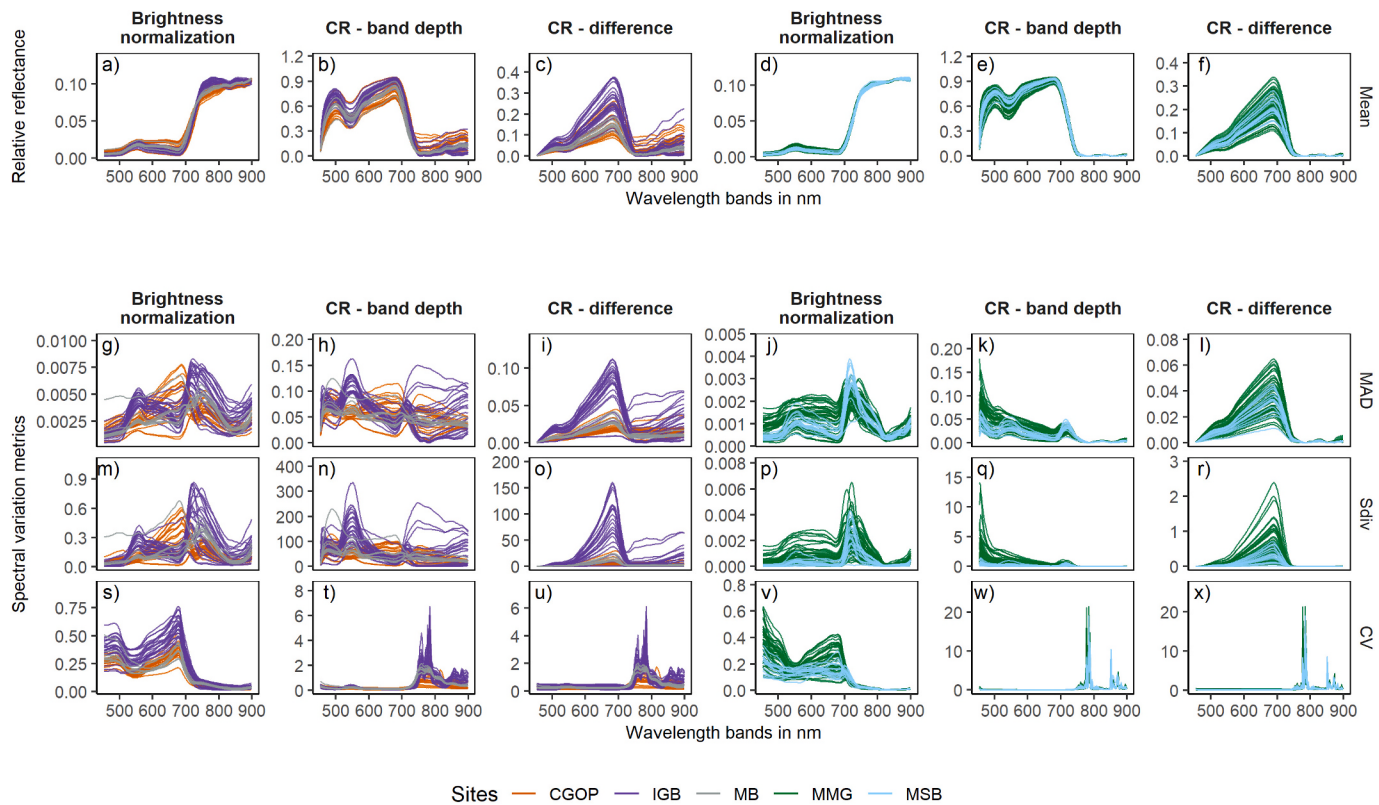


Fig. 4. Spectral reflectance and spectral variation metrics across sites, processing methods, and spectral diversity metrics. The first row (a–f) shows **mean reflectance spectra** for each plot after applying brightness normalization or continuum removal (CR – band depth, CR – difference). Subsequent rows display different **spectral variation metrics**: mean absolute deviation (MAD; g–l), spectral diversity (Sdiv; m–r), and coefficient of variation (CV; s–x). Reflectance spectra are unitless (relative reflectance), while spectral variation metrics are dimensionless except for the coefficient of variation (CV), which is normally expressed as a percentage. Colors represent different study sites. Panels are organized by spectral correction methods (columns) and spectral metric (rows).

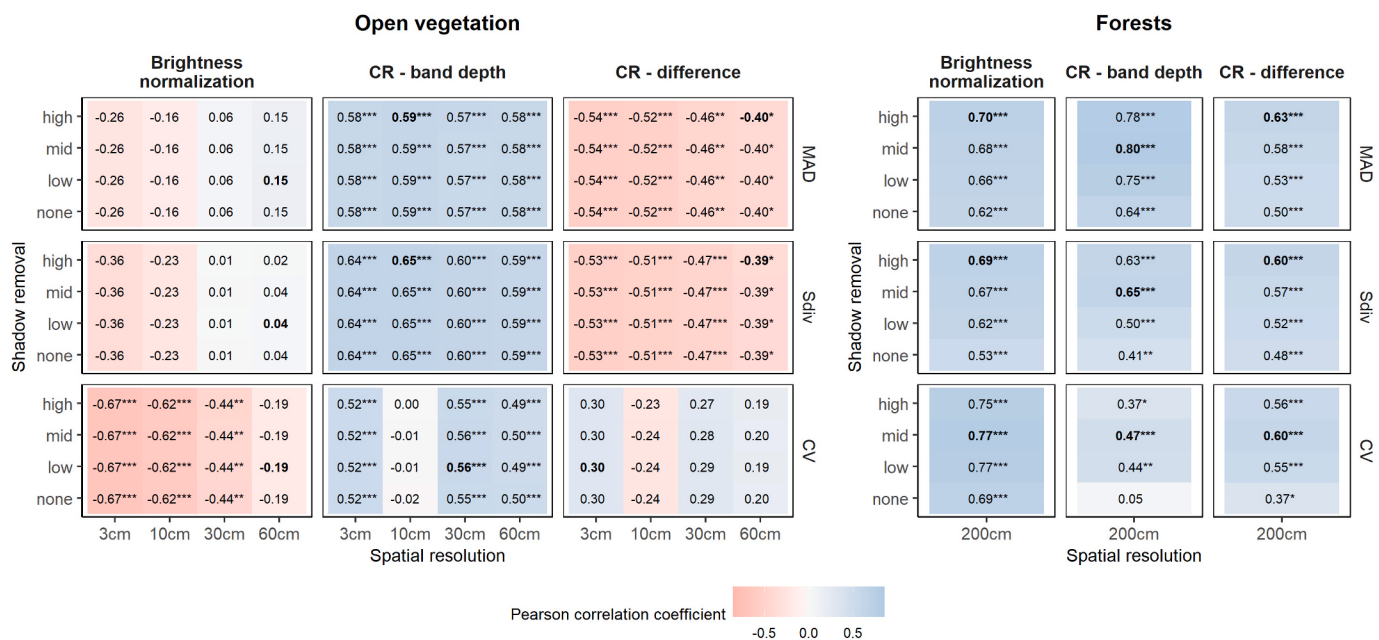


Fig. 5. Pearson correlation coefficient for the relationship of functional dispersion of plants and spectral diversity based on different pixel sizes, processing methods and spectral diversity metrics. For forests no spatial resampling has been done. To enhance comparability, the same plots were used for all combinations ($n = 44$ for open vegetation, $n = 49$ for forests). Bold values indicate the highest Pearson correlation coefficient within each set of illumination corrections and spectral diversity metric. Significance of correlations is indicated with * for $p < 0.1$, ** for $p < 0.01$, and *** for $p < 0.001$.

3.3. Spectral-plant diversity relationships across and within sites

To further examine the contrasting positive and negative relationships highlighted in previous figures, we tested specific combinations of pixel sizes, correction methods, and shadow filtering effects on spectral-plant diversity relationships across and within vegetation sites (Fig. 6; see also Fig. S7 for 10 cm pixel size). The relationships that initially appeared negative across all open vegetation sites using brightness normalized spectral diversity or spectral diversity based on CR – difference in Fig. 5 mostly show neutral or positive relationships when analyzed within individual sites (Fig. 6 a, g, m, c, i, o). Relationships between CV and plant functional diversity in within-site analyses were partly negative irrespective of the illumination correction (Fig. 6 m, n, o).

Exploring wavelength-band-specific relationships showed that the spectral regions with peaks in spectral variation (Fig. 4) are not necessarily those with positive relationships to plant functional diversity (Fig. 7). For continuum removal, the greatest positive correlations were found between 600 and 700 nm, followed by the spectral regions around 500 nm and 750 nm in open vegetation, and 550 nm and 850 in forests, respectively (Fig. 7 columns 2, 3, 5, 6). In contrast, spectral diversity derived from brightness normalized spectra showed peaks around 500 nm and between 600 and 700 nm for all spectral diversity metrics despite CV (Fig. 7 columns 1, 4).

4. Discussion

We investigated how various methodological decisions impact the application of the SVH across different ecosystems and sites. Our findings reveal that spectral diversity metrics are significantly influenced by

factors such as spatial resolution, shadow removal thresholds, and spectral transformations. Specifically, we observed that illumination correction techniques have strong effects on spectral data, with each method emphasizing different spectral features.

Notably, we found negative relationships between spectral and plant functional diversity across open vegetation sites when brightness normalization or continuum removal based on subtraction was applied, in contrast to positive relationships observed with continuum removal using band depth. These results underscore the difficulty of assessing the generality of relationships between spectral and functional plant diversity, highlighting a critical role of methodological decisions in shaping observed relationships. Ultimately, our findings suggest that the utility of SVH in assessing biodiversity is highly dependent on methodological choices, which could lead to varying or even contradictory interpretations of biodiversity patterns. It is therefore essential to establish clear guidelines for selecting and applying these methods, taking into account specific characteristics of the study ecosystem and assessing the necessity for corrections that modify spectra beyond the required basic preprocessing (i.e., radiometric and atmospheric). The variability in results due to different processing steps suggests that without such guidance, the SVH may lead to inconsistent or misleading conclusions.

4.1. Illumination corrections

Standardizing hyperspectral data acquired under varying illumination conditions is crucial for making comparisons both within and across sites when applying analytical methods that are sensitive to such variation. In addition, previous studies have indicated that BRDF (Bidirectional Reflectance Function) effects (not evaluated here)

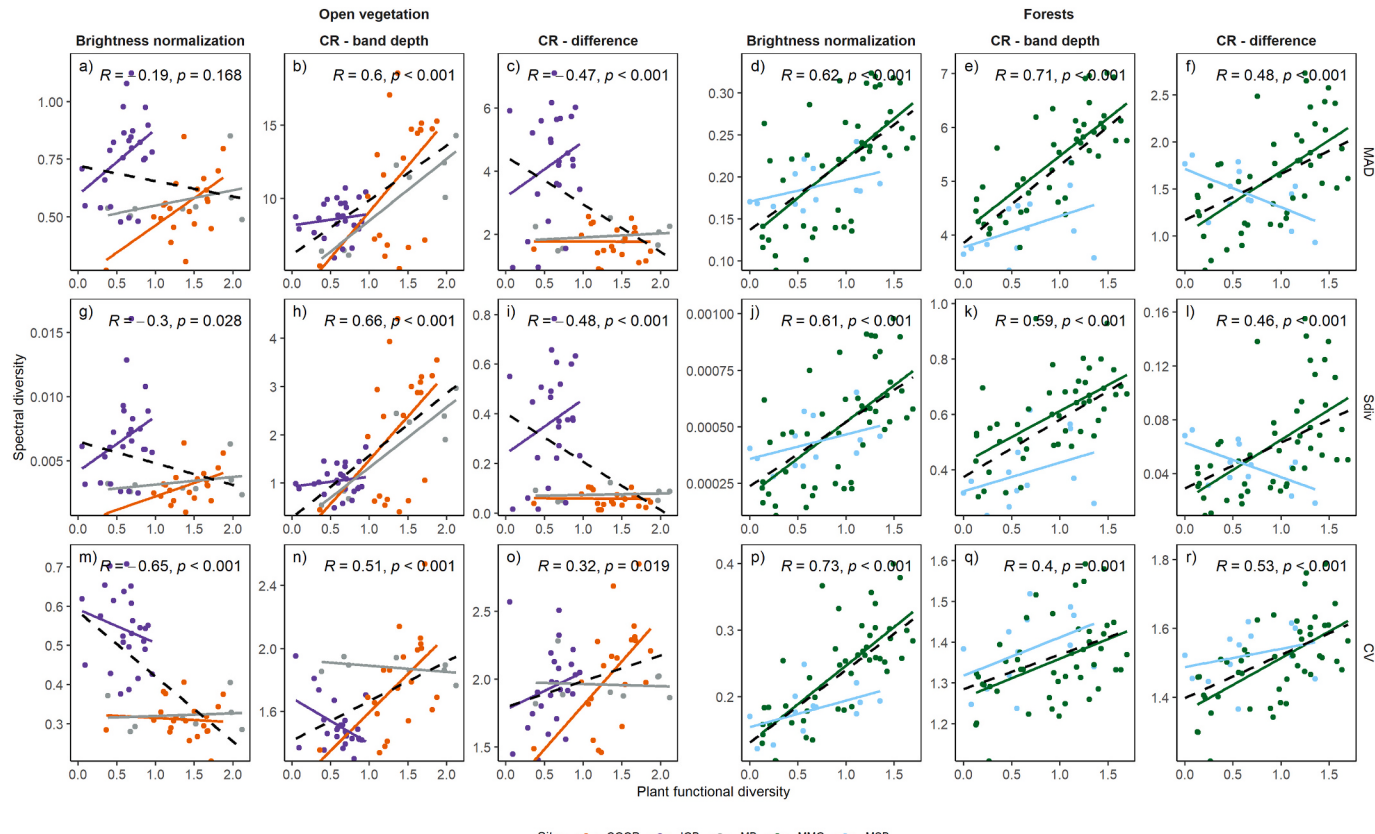


Fig. 6. Scatterplots of plant functional dispersion and spectral diversity metrics based on either brightness normalization or continuum removal (band depth or difference). Shadows were filtered using the mid threshold and in open vegetation raster images at a pixel size of 3 cm were used resulting in 54 plots for open vegetation and 60 plots for forests. Dashed black line indicates the fit across all included sites. Colored straight lines indicate the fit of within site correlations. The Pearson correlation coefficient and *p*-values are given for the across site correlations.

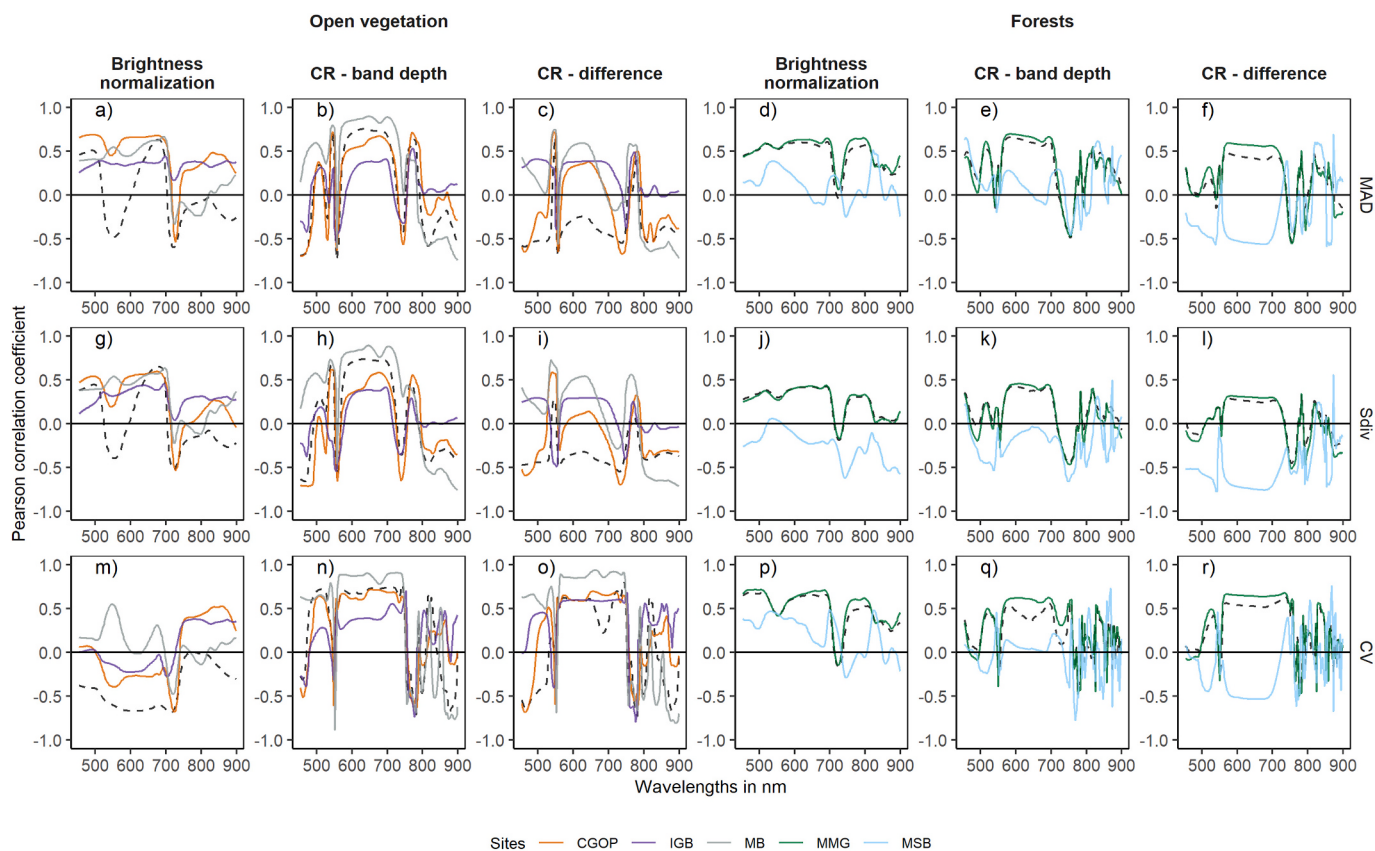


Fig. 7. Pearson correlation coefficients between plant functional dispersion and spectral diversity, calculated for individual wavelength bands for each site, as well as for all open vegetation and forests (dashed black line). Corresponding results using Spearman's rho and Kendall's tau are provided in Supplementary Fig. 8 and 9.

and varying illumination conditions can significantly impact model results: [Rossi et al. \(2022\)](#), for instance, reported a negative relationship between plant species richness and spectral diversity metrics, attributing this to BRDF effects where high biomass plots with low species richness led to heterogeneous light scattering patterns and higher spectral diversity. [Arroyo-Mora et al. \(2021\)](#) suggested that diffuse illumination conditions could mitigate these effects, although acquiring hyperspectral data across consistently diffuse illumination conditions, both within and across sites, is logistically challenging.

A universal approach for illumination correction is still debated, as the effectiveness of different methods can vary depending on the metrics and applications involved. In our study, we examined two pixel-wise spectral transformations—brightness normalization and continuum removal—both of which have been used in previous ecology-driven studies of the SVH ([Crofts et al., 2024a](#); [Féret and Asner, 2014](#); [Schweiger and Laliberté, 2022](#); [Wallis et al., 2023](#)). [Imran et al. \(2021\)](#) found that continuum removal improved the correlation between variance-based spectral diversity metrics and plant diversity compared to no prior spectral transformation. Similarly, [Liu et al. \(2023\)](#) showed that brightness normalization enhanced data consistency within individual crowns and improved differentiation between crowns, which was beneficial for modeling canopy foliar photosynthetic capacity.

Directional effects in airborne pushbroom hyperspectral imagery, such as those arising from varying off-nadir viewing angles, may influence apparent reflectance. In our dataset, viewing angles ranged up to $\sim 20^\circ$ (Fig. S2), with site-level means generally below 10° —a range that is typical and operationally necessary.

Importantly, illumination geometry-related reflectance variation is strongly influenced by ground cover and the relative viewing geometry of the sensor and solar illumination (e.g., flying into or perpendicular to the sun) ([Kalacska et al., 2018](#)), more so than by modest viewing angle

deviations alone. While current hyperspectral satellite missions (e.g., DESIS $\pm 15^\circ$, EnMAP up to $\pm 30^\circ$) operate within similar angular ranges, the geometry of observation in relation to illumination from low-flying airborne platforms becomes an important consideration which must also be weighted by operational and logistical constraints. Nonetheless, such angular variability remains a realistic source of non-ecological spectral variation, and future work should also consider evaluation of BRDF effect and correction strategies when feasible.

In addition, although standard atmospheric correction was applied using ATCOR-4, residual atmospheric features remain visible in some pixel reflectance spectra as expected (Fig. S1). This is a known limitation of radiation transfer-based models, which are often parameterized using standard atmospheres and do not fully capture real-world variability in atmospheric composition and conditions. As such, minor residual artifacts are expected, particularly in absorption bands associated with water vapor, carbon dioxide, oxygen and other atmospheric constituents. While such effects can introduce some uncertainty in spectral reflectance, their influence is likely modest compared to the primary methodological factors considered in this study. It is important for users of such data to be aware of the wavelength regions affected by various atmospheric constituents to ensure those residual features are not used in further analysis. In most hyperspectral workflows, these regions are typically masked or excluded from downstream analysis. More advanced correction approaches—such as localized calibration using reflectance panels or on-site atmospheric column characterization with radiosondes, dropsondes, and atmospheric composition sensors followed by more detailed modeling via tools like 6S or MODTRAN—can reduce these residuals but are often not operationally feasible. We note that minimizing such non-ecological variation remains an important goal for improving comparability in spectral diversity studies.

These effects are especially relevant in spectral diversity studies,

where it is essential to minimize non-ecological influences and preserve ecologically meaningful variance. More advanced approaches, such as those utilizing kernel-based bidirectional reflectance correction, are considered standard in many hyperspectral workflows (Pokrovsky and Roujeau, 2003), potentially addressing illumination effects more comprehensively than pixel-wise transformations.

While the illumination correction methods we tested varied in their ability to standardize spectral signals, their performance was not uniform across ecosystems. In the following section, we examine how vegetation structure and context influenced these results.

4.2. Comparability across sites and ecosystem types

We included both forest and open vegetation sites to evaluate how spectral–plant diversity relationships respond to methodological choices across ecosystems that differ in structure, composition, and spatial scale. For spectral diversity, we found positive relationships within individual open vegetation sites using the MAD and Sdiv metrics. However, across open vegetation sites, these relationships weakened or became slightly negative when brightness-normalized spectra were used. In contrast, continuum removal based on band depth yielded consistently positive relationships across all sites and methods. This suggests that brightness normalization alone does not sufficiently standardize spectral information for comparisons across heterogeneous open ecosystems. As noted by Feilhauer et al. (2010), brightness normalization only partially corrects for variability caused by factors such as LAI and viewing geometry.

Forest sites showed more consistent relationships across all pre-processing methods. This likely reflects their more uniform canopy structure and lower variability in background effects, which reduce methodological sensitivity. Although only one of the forest sites (MMG) was topographically corrected, both forest sites yielded comparable results, suggesting that topographic correction had limited impact relative to the overall structural homogeneity of forest canopies. Still, spectral diversity metrics based on band depth produced stronger and more stable relationships than those based on subtraction or brightness normalization, even in the forest data. Stronger relationships observed at MMG may also reflect ecological drivers, including a clear elevational gradient and associated turnover in species and traits (Wallis et al., 2024). A controlled comparison of the effects of topographic correction was not possible, as uncorrected imagery was unavailable for MMG. While MSB could be considered a reference, its flatter topography and lower functional diversity limited its value for comparison. Nonetheless, our results suggest that topographic correction may enhance comparability in structurally complex terrain when paired with robust spectral normalization.

In summary, our results revealed a striking difference between forests and open vegetation. Not only were correlations between spectral and functional diversity generally weaker in open vegetation but in some cases they were even negative. These findings are consistent with previous work showing that the performance of spectral diversity metrics depends on canopy structure, plant size relative to pixels, and LAI (Schweiger and Laliberté, 2022). As discussed in Torresani et al. (2024), these ecosystem-level characteristics introduce uncertainties that complicate efforts to define a universal implementation of the SVH. Viewed from above, forests in our region appear largely uniform in spectral properties, dominated by live foliage despite some variation in illumination and shading. This spectral uniformity likely enhances the performance of the SVH in forested systems. In contrast, open vegetation includes more visible dead biomass, bare ground, non-vascular plants or lichens, as well as a larger diversity of plant architectures and leaf morphologies. These features contribute to spectral complexity and subpixel heterogeneity, especially when individual plants are smaller than the pixel resolution or pixel size. Importantly, our forest sites were imaged using airborne sensors with coarser spatial resolution and larger pixel size (2 m), while the open vegetation sites were surveyed using a UAV-based sensor at finer resolution and smaller pixel size (3 cm). This

difference in scale was appropriate for each ecosystem, but it may also contribute to the observed differences in SVH performance, as smaller pixels tend to capture greater within-site spectral variation and are more sensitive to effects such as shadowing. Even the small pixels in open vegetation are more likely to include mixtures of species and non-vegetated elements than in forests (Gholizadeh et al., 2018), which may reduce the strength and consistency of SVH relationships across such heterogeneous sites. Thus, caution is needed when interpreting cross-ecosystem comparisons that also differ in spatial scale. Our results suggest that open vegetation sites are more sensitive to methodological choices due to their greater structural and spectral heterogeneity. While this presents challenges for SVH applications, our findings also show that appropriate preprocessing methods—particularly band depth correction—can improve comparability across sites and ecosystem types.

4.3. Combined effects of spectral transformations, spectral diversity metrics and spectral regions

While we showed that the two investigated illumination corrections can have a major impact on spectral-plant functional diversity relationships, we also identified that they impacted the shape of the reflectance data, their spectral diversity and the most important wavelength band regions for predicting plant functional diversity.

Brightness normalization maintained the characteristic spectral shape, reducing the magnitude of values without altering the relative differences between bands. However, the spectral regions with peaks of variation (MAD and Sdiv) among open vegetation sites differed notably when brightness normalization was used compared to continuum removal. Continuum removal using band depth and difference emphasized two absorption features around 450 nm and 650 nm, resulting in more uniform spectral diversity metrics across all wavelength bands and sites. This method significantly altered the spectral pattern by emphasizing the VIS spectrum and reducing values in the NIR, potentially offering a more balanced view of spectral diversity across spectral regions. These differences in spectral patterns highlight the sensitivity of spectral diversity metrics to preprocessing methods. However, it has also been argued that metrics relying on first-order statistics or those influenced by spectral amplitude over shape may be less effective for certain applications (Landgebe, 2002).

The coefficient of variation (CV) from continuum-removed spectra did not exhibit the same clear spectral regions as observed with MAD and SDiv metrics (Fig. 4n versus Fig. 4f,b). This discrepancy likely arises because CV is standardized to the mean, which often approaches zero after continuum removal, making CV values unstable. However, when examining band-wise correlations (Fig. 6j for CV compared to Fig. 6f for MAD and Fig. 6b for SDiv), we find that the spectral regions with high correlations (i.e., informative wavelengths) largely overlap across all three metrics. Specifically, the same peaks in the near-infrared (around 750–850 nm) and red-edge regions (around 700–730 nm) are apparent. This overlap indicates that, despite the biases observed at the full-spectrum metric level (e.g., in Fig. 4n), CV from continuum-removed spectra still captures meaningful ecological variation when examined at the band level. Thus, CV remains an informative metric for capturing spectral diversity patterns, especially when focusing on specific wavelength regions.

We found that the importance of spectral regions depended on the illumination correction applied. High correlations with plant functional diversity were found in the red part of the spectrum, particularly within open vegetation sites, supporting the findings of previous studies (Gholizadeh et al., 2018; Imran et al., 2021). Similarly, high correlations were found in forested areas when both forest sites were considered. It is important to note that these findings are based on the specific correction methods and analytical approaches used in this study. Other techniques, such as feature extraction or shape metrics, may yield different patterns of spectral importance. Additionally, important spectral regions might also differ across spatial resolutions, as identified by Gholizadeh et al.

(2018), adding further complexity which was not tested here.

Overall, while spectral diversity metrics and specific spectral regions provide valuable insights, the choice of preprocessing methods and the spectral regions emphasized can significantly influence the outcomes of spectral-plant diversity approaches. Therefore, the selection of preprocessing techniques and the spectral regions emphasized are not just methodological choices but critical determinants of the accuracy and reliability of spectral-plant diversity assessments, directly shaping the ecological insights derived from remote sensing data.

4.4. Spatial resolution and shadow filtering

In our study, finer spatial resolutions (pixel size of 3–30 cm) were essential for accurately capturing the heterogeneity of plant species and their spectral signatures in open vegetation sites. Coarser resolutions, here 60 cm, showed a decrease in the model fit of most plant-spectral diversity relationships (Fig. 4). At this spatial resolution, mixed pixels likely obscure the spectral characteristics of individual species, thereby compromising the reliability of spectral diversity metrics. These findings confirm prior studies indicating the importance of matching spatial resolution with the scale of the target vegetation to improve the precision of biodiversity assessments (Rossi et al., 2022; Wang et al., 2018).

We employed a relatively simple shadow removal technique that is commonly used in studies of various ecosystems (e.g., Badourdine et al., 2023; Schweiger and Laliberté, 2022). However, this approach relies on subjective visual interpretation of shadowed pixels, which could affect its effectiveness. Compared to other methodological effects explored in this study, the three different thresholds for shadow masking had a relatively minor impact on the relationships between spectral diversity and plant functional diversity. This is in contrast to previous studies that highlighted shadows as a confounding effect on spectral analysis and as an important methodological step when working with (hyper-)spectral data (Adeline et al., 2013; Milas et al., 2017; Rüfenacht et al., 2014; Zhang et al., 2015). Lopatin et al. (2019) recommend minimizing shadow effects during analysis, as even with calibration, misclassification rates of vegetation classes in shadowed areas can reach up to 100 %. While more advanced methods like deep learning could reduce shadow-related errors, Lopatin et al. (2019) suggest that pre-processing to remove shadows remains essential. For UAV-based data collection, acquisition around solar noon (~13:00 local time) is recommended to limit shadow interference. However, given the broad spatial coverage and the associated costs of UAV campaigns, data collection often spans multiple days and times, making shadow minimization during data collection challenging.

While large shadows were removed using reflectance thresholds in our study, many pixels likely contain some level of subpixel shadowing, and inscattering even under near-optimal light conditions. These small-scale shadows are harder to detect but may still influence spectral variation in ways unrelated to vegetation. Recent approaches such as object-based spectral unmixing offer potential for addressing this issue more precisely (Zhang et al., 2025), though their use in biodiversity studies is still emerging. Continued development and testing of such approaches could improve the robustness of spectral diversity metrics in high-resolution imaging spectroscopy.

5. Conclusion

This study underscores the crucial role of methodological choices in spectral diversity assessments and their connection to plant functional diversity. Our results demonstrate that different illumination corrections, spectral diversity metrics, and wavelength regions significantly influence spectral diversity's rank-order across sites and its relation to plant functional diversity, while spatial resolution and shadow filtering have a lesser but still important effect. The variability observed in spectral diversity across diverse ecosystems, especially in open vegetation sites, underscores the challenges of disentangling the effects of

brightness and trait variation. The findings suggest that careful consideration of these methodological aspects is crucial for accurate spectral diversity assessments. We need to ask which information is ecologically driven and which is due to non-ecological effects. To enhance remote sensing applications and improve biodiversity monitoring, future research should focus on standardizing hyperspectral data across sites and sensors, addressing the complexities introduced by illumination and spectral processing methods.

CRediT authorship contribution statement

Christine I.B. Wallis: Writing – review & editing, Writing – original draft, Visualization, Validation, Resources, Methodology, Investigation, Formal analysis, Conceptualization. **Anna L. Crofts:** Writing – review & editing, Data curation, Conceptualization. **Robert Jackisch:** Visualization, Formal analysis, Writing – review & editing. **Shan Kothari:** Writing – review & editing, Data curation. **Guillaume Tougas:** Writing – review & editing, Data curation, Visualization. **J. Pablo Arroyo-Mora:** Writing – review & editing, Data curation. **Paul Hacker:** Writing – review & editing. **Nicholas Coops:** Writing – review & editing. **Margaret Kalacska:** Writing – review & editing, Data curation. **Etienne Laliberté:** Writing – review & editing, Funding acquisition. **Mark Vellend:** Writing – review & editing, Project administration, Methodology, Data curation, Conceptualization, Funding acquisition, Resources.

Declaration of competing interest

The authors declare that they have no known competing financial interests or personal relationships that could have appeared to influence the work reported in this paper.

Acknowledgements

This study was conducted in the framework of the Canadian Airborne Biodiversity Observatory (CABO) project, funded by the Natural Sciences and Engineering Research Council of Canada (509190-2017). We would like to thank the many field and laboratory assistants for their help in conducting the plant inventory surveys and leaf sampling, and in quantifying foliar traits. In particular, we would like to recognize Sabrina Demers-Thibeault who led the leaf sampling and foliar trait quantification effort as well as the team that processed the hyperspectral imagery, including Deep Inamdar. We additionally would like to thank Raymond Soffer from the National Research Council Canada (NRC) for his help with the preprocessing of the hyperspectral data. We thank the staff in Parc national du Mont Mégantic, Parc national du Mont-Saint-Bruno, Parc national des îles-de-Boucherville, and the Cowichan Garry Oak Preserve for facilitating access to the field sites and their ongoing support. We are grateful to the associate editor and three anonymous reviewers for their constructive feedback, which significantly improved the quality of this manuscript.

Appendix A. Supplementary data

Supplementary data to this article can be found online at <https://doi.org/10.1016/j.rse.2025.114907>.

Data availability

Inventory data and the corresponding R code are available on Zenodo: <https://doi.org/10.5281/zenodo.15868769>.

References

- Adeline, K.R.M., Chen, M., Briottet, X., Pang, S.K., Paparoditis, N., 2013. Shadow detection in very high spatial resolution aerial images: a comparative study. *ISPRS J. Photogramm. Remote Sens.* 80, 21–38. <https://doi.org/10.1016/j.isprsjprs.2013.02.003>.

- Arroyo-Mora, J.P., Kalacska, M., Inamdar, D., Soffer, R., Lucanus, O., Gorman, J., Naprstek, T., Schaaf, E.S., Ifimov, G., Elmer, K., Leblanc, G., 2019. Implementation of a UAV-hyperspectral Pushbroom imager for ecological monitoring. *Drones* 3, 12. <https://doi.org/10.3390/drones3010012>.
- Arroyo-Mora, J.P., Kalacska, M., Løke, T., Schläpfer, D., Coops, N.C., Lucanus, O., Leblanc, G., 2021. Assessing the impact of illumination on UAV pushbroom hyperspectral imagery collected under various cloud cover conditions. *Remote Sens. Environ.* 258, 112396. <https://doi.org/10.1016/j.rse.2021.112396>.
- Ayotte, J., Laliberté, E., 2019. Measuring Leaf Carbon Fractions with the ANKOM2000 Fiber Analyzer.
- Badourdinne, C., Féret, J.-B., Pélissier, R., Vincent, G., 2023. Exploring the link between spectral variance and upper canopy taxonomic diversity in a tropical forest: influence of spectral processing and feature selection. *Remote Sens. Ecol. Conserv.* 9, 235–250. <https://doi.org/10.1002/rse2.306>.
- Behmann, J., Mahlein, A.-K., Paulus, S., Dupuis, J., Kuhlmann, H., Oerke, E.-C., Plümer, L., 2016. Generation and application of hyperspectral 3D plant models: methods and challenges. *Mach. Vis. Appl.* 27, 611–624. <https://doi.org/10.1007/s00138-015-0716-8>.
- Cavender-Bares, J., Gamon, J.A., Hobbie, S.E., Madritch, M.D., Meireles, J.E., Schweiger, A.K., Townsend, P.A., 2017. Harnessing plant spectra to integrate the biodiversity sciences across biological and spatial scales. *Am. J. Bot.* 104, 966–969. <https://doi.org/10.3732/ajb.1700061>.
- Chang, C.-I., 2000. An information-theoretic approach to spectral variability, similarity, and discrimination for hyperspectral image analysis. *Inf. Theory IEEE Trans. On* 46, 1927–1932. <https://doi.org/10.1109/18.857802>.
- Clark, R.N., Roush, T.L., 1984. Reflectance spectroscopy: quantitative analysis techniques for remote sensing applications. *J. Geophys. Res. Solid Earth* 89, 6329–6340. <https://doi.org/10.1029/JB089iB07p06329>.
- Conti, L., Malavasi, M., Galland, T., Komárek, J., Lagner, O., Carmona, C.P., de Bello, F., Rocchini, D., Šimová, P., 2021. The relationship between species and spectral diversity in grassland communities is mediated by their vertical complexity. *Appl. Veg. Sci.* 24. <https://doi.org/10.1111/avsc.12600>.
- Coops, N.C., Tompalski, P., Goodbody, T.R.H., Achim, A., Mulverhill, C., 2023. Framework for near real-time forest inventory using multi source remote sensing data. *For. Int. J. For. Res.* 96, 1–19. <https://doi.org/10.1093/forestry/cpac015>.
- Crofts, A.L., St-Jean, S., Vellend, M., 2022. Canadian Airborne Biodiversity Observatory's Forest Inventory Field Survey Protocol.
- Crofts, A., Wallis, C., St-Jean, S., Demers-Thibeault, S., Inamdar, D., Arroyo, P., Kalacska, M., Laliberté, E., Vellend, M., 2024a. Linking aerial hyperspectral data to canopy tree biodiversity: An examination of the spectral variation hypothesis. <https://doi.org/10.1002/ecm.1605>.
- Crofts, A., Wallis, C., St-Jean, S., Demers-Thibeault, S., Inamdar, D., Arroyo-Mora, J.P., Kalacska, M., Laliberté, E., Vellend, M., 2024b. CABO Forest Inventory Survey Data: Canopy-Level Spectra, Species Abundances, and Environmental Conditions. <https://doi.org/10.5061/DRYAD.5MKKWH7DH>.
- Dahlin, K.M., 2016. Spectral diversity-area relationships for assessing biodiversity in a wildland-agriculture matrix. *Ecol. Appl. Publ. Ecol. Soc. Am.* 26, 2756–2766. <https://doi.org/10.1002/eap.1390>.
- Eismann, M., 2012. Spectral Data Models PM210, 503–563. <https://doi.org/10.1117/3.899758.ch12>.
- Elmer, K., Kalacska, M., Arroyo-Mora, J.P., 2021. Mapping the extent of invasive Phragmites australis subsp. australis from airborne hyperspectral imagery. *Front. Environ. Sci.* 9. <https://doi.org/10.3389/fenvs.2021.757871>.
- Fassnacht, F.E., Müllerová, J., Conti, L., Malavasi, M., Schmidlein, S., 2022. About the link between biodiversity and spectral variation. *Appl. Veg. Sci.* 25, e12643. <https://doi.org/10.1111/avsc.12643>.
- Feilhauer, H., Asner, G.P., Martin, R.E., Schmidlein, S., 2010. Brightness-normalized partial least squares regression for hyperspectral data. *J. Quant. Spectrosc. Radiat. Transf.* 111, 1947–1957. <https://doi.org/10.1016/j.jqsrt.2010.03.007>.
- Féret, J.-B., Asner, G.P., 2014. Mapping tropical forest canopy diversity using high-fidelity imaging spectroscopy. *Ecol. Appl.* 24, 1289–1296. <https://doi.org/10.1890/13-1824.1>.
- Frye, H.A., Aiello-Lammens, M.E., Euston-Brown, D., Jones, C.S., Kilroy Mollmann, H., Merow, C., Slingsby, J.A., van der Merwe, H., Wilson, A.M., Silander Jr., J.A., 2021. Plant spectral diversity as a surrogate for species, functional and phylogenetic diversity across a hyper-diverse biogeographic region. *Glob. Ecol. Biogeogr.* 30, 1403–1417. <https://doi.org/10.1111/geb.13306>.
- Gholizadeh, H., Gamon, J.A., Zygielbaum, A.I., Wang, R., Schweiger, A.K., Cavender-Bares, J., 2018. Remote sensing of biodiversity: soil correction and data dimension reduction methods improve assessment of α -diversity (species richness) in prairie ecosystems. *Remote Sens. Environ.* 206, 240–253. <https://doi.org/10.1016/j.rse.2017.12.014>.
- Girard, A., Schweiger, A.K., Carteron, A., Kalacska, M., Laliberté, E., 2020. Foliar spectra and traits of bog plants across nitrogen deposition gradients. *Remote Sens.* 12, 2448. <https://doi.org/10.3390/rs12152448>.
- Goetz, S., Dubayah, R., 2011. Advances in remote sensing technology and implications for measuring and monitoring forest carbon stocks and change. *Carbon Manag.* 2, 231–244. <https://doi.org/10.4155/cmt.11.18>.
- Grubinger, S., Coops, N.C., O'Neill, G.A., 2023. Picturing local adaptation: spectral and structural traits from drone remote sensing reveal clinal responses to climate transfer in common-garden trials of interior spruce (*Picea engelmannii* × *glauca*). *Glob. Chang. Biol.* 29, 4842–4860. <https://doi.org/10.1111/gcb.16855>.
- Hacker, P., Coops, N., Laliberté, E., Michaletz, S., 2022. Variations in accuracy of leaf functional trait prediction due to spectral mixing. *Ecol. Indic.* 136, 108687. <https://doi.org/10.1016/j.ecolind.2022.108687>.
- Huete, A.R., 2004. 11 - REMOTE SENSING FOR ENVIRONMENTAL MONITORING. In: Artiola, J.F., Pepper, I.L., Brusseau, M.L. (Eds.), *Environmental Monitoring and Characterization*. Academic Press, Burlington, pp. 183–206. <https://doi.org/10.1016/B978-012064477-3/50013-8>.
- Imran, H.A., Gianelle, D., Scotton, M., Rocchini, D., Dalponte, M., Macolino, S., Sakowska, K., Pornaro, C., Vescovo, L., 2021. Potential and limitations of grasslands α -diversity prediction using fine-scale hyperspectral imagery. *Remote Sens.* 13, 2649. <https://doi.org/10.3390/rs13142649>.
- Inamdar, D., Kalacska, M., Arroyo-Mora, J.P., Leblanc, G., 2021a. The directly-georeferenced hyperspectral point cloud: preserving the integrity of hyperspectral imaging data. *Front. Remote Sens.* 2. <https://doi.org/10.3389/frsen.2021.675323>.
- Inamdar, D., Kalacska, M., Leblanc, G., Arroyo-Mora, J.P., 2021b. Implementation of the directly-georeferenced hyperspectral point cloud. *MethodsX* 8, 101429. <https://doi.org/10.1016/j.mex.2021.101429>.
- Inamdar, D., Kalacska, M., Darko, P.O., Arroyo-Mora, J.P., Leblanc, G., 2023. Spatial response resampling (SR2): accounting for the spatial point spread function in hyperspectral image resampling. *Methods X* 10. <https://doi.org/10.1016/j.mex.2023.101998>.
- Jacquemoud, S., Ustin, S., 2019. Leaf Optical properties. Cambridge University Press, Cambridge. <https://doi.org/10.1017/978108686457>.
- Jánicek, C., Okujeni, A., Cooper, S., Clark, M., Hostert, P., van der Linden, S., 2020. Brightness gradient-corrected hyperspectral image mosaics for fractional vegetation cover mapping in northern California. *Remote Sens. Lett.* 11, 1–10. <https://doi.org/10.1080/2150704X.2019.1670518>.
- Kattge, J., Bönnisch, G., Díaz, S., Lavorel, S., Prentice, I.C., Leadley, P., Trenthenhahn, S., Werner, G.D.A., Aakala, T., Abedi, M., Acosta, A.T.R., Adamidis, G.C., Adamson, K., Aiba, M., Albert, C.H., Alcántara, J.M., Alcázar C.C., Aleixo, I., Ali, H., Amiaud, B., Ammer, C., Amoroso, M.M., Anand, M., Anderson, C., Anten, N., Antos, J., Apagaua, D.M.G., Ashman, T.-L., Asmar, D.H., Asner, G.P., Aspinwall, M., Atkin, O., Aubin, I., Bastrup-Spohr, L., Bahalkeh, K., Bahn, M., Baker, T., Baker, W.J., Bakker, J.P., Baldocchi, D., Baltzer, J., Banerjee, A., Baranger, A., Barlow, J., Barneche, D.R., Baruch, Z., Bastianelli, D., Battles, J., Bauerle, W., Bauters, M., Bazzato, E., Beckmann, M., Beeckman, H., Beierkuhnlein, C., Bekker, R., Belfry, G., Belluau, M., Belotti, M., Benavides, R., Benomar, L., Berdugo-Lattke, M.L., Berenguer, E., Bergamin, R., Bergmann, J., Bergmann Carlucci, M., Berner, L., Bernhardt-Römermann, M., Bigler, C., Björkman, A.D., Blackman, C., Blanco, C., Blonder, B., Blumenthal, D., Bocanegra-González, K.T., Boeckx, P., Bohlman, S., Böhning-Gaese, K., Boisvert-Marsh, L., Bond, W., Bond-Lamberty, B., Boom, A., Bonman, C.C.F., Bordin, K., Boughton, E.H., Boukili, V., Bowman, D.M.J.S., Bravo, S., Brendel, M.R., Broadley, M.R., Brown, K.A., Bruehlheide, H., Brumrich, F., Bruun, H.H., Bruylants, D., Buchanan, S.W., Bucher, S.F., Buchmann, N., Buitenhof, R., Bunker, D.E., Bürger, J., Burrascano, S., Burslem, D.F.R.P., Butterfield, B.J., Byun, C., Marques, M., Scalón, M.C., Caccianiga, M., Cadotte, M., Cailleret, M., Camac, J., Camarero, J.J., Campany, C., Campetella, G., Campos, J.A., Cano-Arboleda, L., Canullo, R., Carbognani, M., Carvalho, F., Casanovas, F., Castagneryol, B., Catford, J.A., Cavender-Bares, J., Cerabolini, B.E.L., Cervellini, M., Chacón-Madrigal, E., Chapin, K., Chapin, F.S., Chelli, S., Chen, S.-C., Chen, A., Cherubini, P., Chianucci, F., Choat, B., Chung, K.-S., Chytrý, M., Ciccarelli, D., Coll, L., Collins, C.G., Conti, L., Coomes, D., Cornelissen, J.H.C., Cornwell, W.K., Corona, P., Coeyta, M., Craine, J., Craven, D., Cromsigt, J.P.G., Csécserits, A., Cufar, K., Cuntz, M., da Silva, A.C., Dahlin, K.M., Dainese, M., Dalke, I., Dalle Fratte, M., Dang-Le, A.T., Danhelka, J., Dannoura, M., Dawson, S., de Beer, A.J., De Frutos, A., De Long, J.R., Dechant, B., Delagrange, S., Delpierre, N., Derroire, G., Dias, A.S., Diaz-Toribio, M.H., Dimitrakopoulos, P.G., Dobrowolski, M., Doktor, D., Drévojan, P., Dong, N., Dransfield, J., Dressler, S., Duarte, L., Ducouret, E., Dullinger, S., Durka, W., Duursma, R., Dymova, O., E-Vojtkó, A., Eckstein, R.L., Ejtehadi, H., Elser, J., Emilio, T., Engemann, K., Erfanian, M.B., Erfmeier, A., Esquivel-Muelbert, A., Esser, G., Estiarte, M., Domingues, T.F., Fagan, W.F., Fagúndez, J., Falster, D.S., Fan, Y., Fang, J., Farris, E., Fazlioglu, F., Feng, Y., Fernández-Mendez, F., Ferrara, C., Ferreira, J., Fidelis, A., Finegan, B., Firn, J., Flowers, T.J., Flynn, D.F.B., Fontana, V., Forey, E., Forgiarini, C., François, L., Frangipani, M., Frank, D., Frenette-Dussault, C., Freschet, G.T., Fry, E.L., Fyllas, N.M., Mazzochini, G.G., Gachet, S., Gallagher, R., Ganade, G., Ganga, F., García-Palacios, J., Gargaglione, V., Garnier, E., Garrido, J.L., de Gasper, A.L., Gea-Izquierdo, G., Gibson, D., Gillison, A.N., Giroldo, A., Glenshardt, M.-C., Gleason, S., Gliesch, M., Goldberg, E., Gödel, B., Gonzalez-Akre, E., Gonzalez-Andujar, J.L., González-Melo, A., González-Robles, A., Graae, B.J., Granda, E., Graves, S., Green, W.A., Gregor, T., Gross, N., Guerin, G.R., Günther, A., Gutierrez, A.G., Haddock, L., Haines, A., Hall, J., Hambackers, A., Han, W., Harrison, S.P., Hattingh, W., Hawes, J.E., He, T., He, P., Heberling, J.M., Helm, A., Hempel, S., Hentschel, J., Héraut, B., Heres, A.-M., Herz, K., Heuertz, M., Hickler, T., Hietz, P., Higuchi, P., Hipp, A.L., Hirons, A., Hock, M., Hogan, J.A., Holl, K., Honnay, O., Hornstein, D., Hou, E., Hough-Snee, N., Hovstad, K.A., Ichie, T., Igic, B., Illa, E., Isaac, M., Ishihara, M., Ivanov, L., Ivanova, L., Iversen, C.M., Izquierdo, J., Jackson, R.B., Jackson, B., Jacquet, H., Jagodzinski, A.M., Jandt, U., Jansen, S., Jenkins, T., Jentsch, A., Jespersen, J.R.P., Jiang, G.-F., Johansen, J.L., Johnson, D., Jokela, E.J., Joly, C.A., Jordan, G.J., Joseph, G.S., Junaedi, D., Junker, R.R., Justes, E., Kabzemis, R., Kane, J., Kaplan, Z., Kattenborn, T., Kavelenova, L., Kearsley, E., Kempel, A., Kenzo, T., Kerkhoff, A., Khalil, M.I., Kinlock, N.L., Kissling, W.D., Kitajima, K., Kitzberger, T., Kjoller, R., Klein, T., Kleyer, M., Klimešová, J., Klijp, J., Kloeppe, B., Klotz, S., Knops, J.M.H., Kohyama, T., Koike, F., Kollmann, J., Komac, B., Komatsu, K., König, C., Kraft, N.J.B., Kramer, K., Kreft, H., Kühn, I., Kumarathunge, D., Kuppler, J., Kurokawa, H., Kurosawa, Y., Kuyah, S., Laclau, J.-P., Lafleur, B., Lallai, E., Lamb, E., Lampricht, A., Larkin, D.J., Laughlin, D., Le Bagousse-Pinguet, Y., le Maire, G., le Roux, P.C., le Roux, E., Lee, T., Lens, F., Lewis, S.L., Lhotsky, B., Li, Y., Li, X., Lichstein, J.W., Liebergesell, M., Lim, J.Y., Lin, Y.-S., Linares, J.C., Liu, C., Liu, D., Liu, U., Livingstone, S., Llusia, J., Lohbeck, M., López-García, Á., Lopez-Gonzalez, G.,

- Lososová, Z., Louault, F., Lukács, B.A., Lukeš, P., Luo, Y., Lussu, M., Ma, S., Maciel Rabelo Pereira, C., Mack, M., Maire, V., Mäkelä, A., Mäkinen, H., Malhado, A.C.M., Mallik, A., Manning, P., Manzoni, S., Marchetti, Z., Marchino, L., Marcilio-Silva, V., Marcon, E., Marignani, M., Markestijn, L., Martin, A., Martínez-Garza, C., Martínez-Vilalta, J., Mašková, T., Mason, K., Mason, N., Massad, T.J., Masse, J., Mayrose, I., McCarthy, J., McCormack, M.L., McCulloh, K., McFadden, I.R., McGill, B.J., McPartland, M.Y., Medeiros, J.S., Medlyn, B., Meerts, P., Mehrabi, Z., Meir, P., Melo, F.P.L., Mencuccini, M., Meredieu, C., Messier, J., Mészáros, I., Metsaranta, J., Michaletz, S.T., Michelaki, C., Migalina, S., Milla, R., Miller, J.E.D., Minden, V., Ming, R., Mokany, K., Moles, A.T., Molnár V.A., Molofsky, J., Molz, M., Montgomery, R.A., Monty, A., Moravcová, L., Moreno-Martínez, A., Moretti, M., Mori, A.S., Mori, S., Morris, D., Morrison, J., Mucina, L., Mueller, S., Muir, C.D., Müller, S.C., Munoz, F., Myers-Smith, I.H., Myster, R.W., Nagano, M., Naidu, S., Narayanan, A., Natesan, B., Negoita, L., Nelson, A.S., Neuschulz, E.L., Ni, J., Niedrist, G., Nieto, J., Niinemets, Ü., Nolan, R., Nottebrock, H., Nouvellon, Y., Novakovskiy, A., Network, T.N., Nyström, K.O., O'Grady, A., O'Hara, K., O'Reilly-Nugent, A., Oakley, S., Oberhuber, W., Ohtsuka, T., Oliveira, R., Öllerer, K., Olson, M.E., Onipchenko, V., Onoda, Y., Onstein, R.E., Ordóñez, J.C., Osada, N., Ostonen, I., Ottaviani, G., Otto, S., Overbeck, G.E., Ozinga, W.A., Pahl, A.T., Paine, C.E.T., Pakeman, R.J., Papageorgiou, A.C., Parfionova, E., Pärte, M., Patacca, M., Paula, S., Paule, J., Pauli, H., Pausas, J.G., Peco, B., Penuelas, J., Perea, A., Peri, P.L., Petisco-Souza, A.C., Petraglia, A., Petritan, A.M., Phillips, O.L., Pierce, S., Pillar, V.D., Pisek, J., Pomogaybin, A., Poorter, H., Portsmuth, A., Poschlod, P., Potvin, C., Pounds, D., Powell, A.S., Power, S.A., Prinzing, A., Pugliali, G., Pyšek, P., Raever, V., Rammig, A., Ransijn, J., Ray, C.A., Reich, P.B., Reichstein, M., Reid, D.E.B., Réjou-Méchain, M., de Dios, V.R., Ribeiro, S., Richardson, S., Riibak, K., Rillig, M.C., Riviera, F., Robert, E.M.R., Roberts, S., Robroek, B., Roddy, A., Rodrigues, A.V., Rogers, A., Rollinson, E., Rolo, V., Römermann, C., Ronzhina, D., Roscher, C., Rosell, J.A., Rosenfield, M.F., Rossi, C., Roy, D.B., Royer-Tardif, S., Rüger, N., Ruiz-Peinado, R., Rumpf, S.B., Rusch, G.M., Ryo, M., Sack, L., Saldaña, A., Salgado-Negret, B., Salguero-Gómez, R., Santa-Regina, I., Santacruz-García, A.C., Santos, J., Sardans, J., Schamp, B., Scherer-Lorenzen, M., Schleuning, M., Schmid, B., Schmidt, M., Schmitt, S., Schneider, J.V., Schowank, S. D., Schrader, J., Schrödt, F., Schuldt, B., Schurr, F., Selaya Garvitz, G., Semchenko, M., Seymour, C., Sfair, J.C., Sharpe, J.M., Sheppard, C.S., Sheremetiev, S., Shiodera, S., Shipley, B., Shovon, T.A., Siebenkäs, A., Sierra, C., Silva, V., Silva, M., Sitzia, T., Sjöman, H., Slot, M., Smith, N.G., Sodhi, D., Soltis, P., Soltis, D., Somers, B., Sonnier, G., Sørensen, M.V., Sosinski Jr, E.E., Soudzilovskaja, N.A., Souza, A.F., Spasojevic, M., Sperandii, M.G., Stan, A.B., Stegen, J., Steinbauer, K., Stephan, J.G., Sterck, F., Stojanovic, D.B., Strydom, T., Suarez, M.L., Svensson, J.-C., Svitková, I., Svitok, M., Svoboda, M., Swaine, E., Swenson, N., Tabarelli, M., Takagi, K., Tappeiner, U., Tarifa, R., Taugoudeau, S., Tavsanoglu, C., te Beest, M., Tedersoo, L., Thiffault, N., Thom, D., Thomas, E., Thompson, K., Thornton, P.E., Thuiller, W., Tichý, L., Tissue, D., Tjoelker, M.G., Tng, D.Y.P., Tobias, J., Török, P., Tarin, T., Torres-Ruiz, J.M., Tóthmérész, B., Treurnicht, M., Trivellone, V., Trolliet, F., Trotsiuk, V., Tsakalos, J., L., Tsiripidis, I., Tysklin, N., Umehara, T., Usoltsev, V., Vadeboncoeur, M., Vaezi, J., Valladares, F., Vamosi, J., van Bodegom, P.M., van Breugel, M., Van Cleemput, E., van der Weg, M., van der Merwe, S., van der Plas, F., van der Sande, M.T., van Kleunen, M., van Meerbeek, K., Vanderwel, M., Vanselow, K.A., Värvhammar, A., Varone, L., Vasquez Valderrama, M.Y., Vasilev, K., Vellend, M., Veneklaas, E.J., Verbeeck, H., Verheyen, K., Vibrans, A., Vieira, I., Villacís, J., Viole, C., Vivek, P., Wagner, K., Waldram, M., Waldron, A., Walker, A.P., Waller, M., Walther, G., Wang, H., Wang, F., Wang, W., Watkins, H., Watkins, J., Weber, U., Weedon, J.T., Wei, L., Weigelt, P., Weiher, E., Wells, A.W., Wellstein, C., Wenk, E., Westoby, M., Westwood, A., White, P.J., Whitten, M., Williams, M., Winkler, D.E., Winter, K., Womack, C., Wright, I.J., Wright, S.J., Wright, J., Pinho, B.X., Ximenes, F., Yamada, T., Yamaji, K., Yanai, R., Yankov, N., Yguel, B., Zanini, K.J., Zanne, A.E., Zelený, D., Zhao, Y.-P., Zheng Jingming, Zheng, Ji, Ziemińska, K., Zirbel, C.R., Zizka, G., Zo-Bi, I.C., Zotz, G., Wirth, C., 2020. TRY plant trait database – enhanced coverage and open access. *Glob. Chang. Biol.* 26, 119–188. doi:<https://doi.org/10.1111/gcb.14904>.
- Kalacska, M., Arroyo-Mora, J.P., Soffer, R.J., Roulet, N.T., Moore, T.R., Humphreys, E., Leblanc, G., Lucanus, O., Inamdar, D., 2018. Estimating peatland water table depth and net ecosystem exchange: A comparison between satellite and airborne imagery. *Remote Sens.* 10, 687. doi:<https://doi.org/10.3390/rs10050687>.
- Kruse, F.A., Lefkoff, A.B., Boardman, J.W., Heidebrecht, K.B., Shapiro, A.T., Barloon, P. J., Goetz, A.F.H., 1993. The spectral image processing system (SIPS)—interactive visualization and analysis of imaging spectrometer data. *Remote Sens. Environ. Airbone Imag. Spectr.* 44, 145–163. doi:[https://doi.org/10.1016/0034-4257\(93\)90013-N](https://doi.org/10.1016/0034-4257(93)90013-N).
- Laliberté, E., 2018. Measuring Specific Leaf Area and Water Content.
- Laliberté, E., Legendre, P., 2010. A distance-based framework for measuring functional diversity from multiple traits. *Ecology* 91, 299–305. doi:<https://doi.org/10.1890/08-2244.1>.
- Laliberté, E., Legendre, P., Shipley, B., 2014. FD: measuring functional diversity from multiple traits, and other tools for functional ecology. R Package Version 1, 0–12.
- Laliberté, E., Schweiger, A.K., Legendre, P., 2020. Partitioning plant spectral diversity into alpha and beta components. *Ecol. Lett.* 23, 370–380. doi:<https://doi.org/10.1111/ele.13429>.
- Landgrebe, D., 2002. Hyperspectral image data analysis. *IEEE Signal Process. Mag.* 19, 17–28. doi:<https://doi.org/10.1109/79.974718>.
- Leboeuf, A., Pomerleau, I., 2015. Province-Wide LiDAR Data Acquisition: Impact Analysis and Recommendations. Ministère des forêts, de la faune et des parcs (MFFP) du Québec, Direction.
- Lehnert, L.W., Meyer, H., Obermeier, W.A., Silva, B., Regeling, B., Bendix, J., 2019. Hyperspectral data analysis in R: the hsdar package. *J. Stat. Softw.* 89, 1–23. doi:<https://doi.org/10.18637/jss.v089.i12>.
- Liu, S., Yan, Z., Wang, Z., Serbin, S., Visser, M., Zeng, Y., Ryu, Y., Su, Y., Guo, Z., Song, G., Wu, Q., Zhang, H., Cheng, K.H., Dong, J., Hau, B.C.H., Zhao, P., Yang, X., Liu, L., Rogers, A., Wu, J., 2023. Mapping foliar photosynthetic capacity in subtropical and tropical forests with USAS-based imaging spectroscopy: scaling from leaf to canopy. *Remote Sens. Environ.* 293, 113612. doi:<https://doi.org/10.1016/j.rse.2023.113612>.
- Lopatin, J., Fassnacht, F., Kattenborn, T., Schmidlein, S., 2017. Mapping plant species in mixed grassland communities using close range imaging spectroscopy. *Remote Sens. Environ.* 201, 12–23. doi:<https://doi.org/10.1016/j.rse.2017.08.031>.
- Lopatin, J., Dolos, K., Kattenborn, T., Fassnacht, F.E., 2019. How canopy shadow affects invasive plant species classification in high spatial resolution remote sensing. *Remote Sens. Ecol. Conserv.* 5, 302–317. doi:<https://doi.org/10.1002/rse2.109>.
- Lopes, M., Fauvel, M., Ouin, A., Girard, S., 2017. Spectro-temporal heterogeneity measures from dense high spatial resolution satellite image time series: application to grassland species diversity estimation. *Remote Sens.* 9, 993. doi:<https://doi.org/10.3390/rs9100993>.
- Manea, D., Calin, M.A., 2015. Hyperspectral imaging in different light conditions. *Imag. Sci. J.* 63, 214–219. doi:<https://doi.org/10.1179/1743131X15Y.0000000001>.
- Milas, A.S., Arend, K., Mayer, C., Simonson, M.A., Mackey, S., 2017. Different colours of shadows: classification of UAV images. *Int. J. Remote Sens.* 38, 3084–3100. doi:<https://doi.org/10.1080/01431161.2016.1274449>.
- Obermeier, W.A., Lehnert, L.W., Pohl, M.J., Makowski Gianonni, S., Silva, B., Seibert, R., Laser, H., Moser, G., Müller, C., Luterbacher, J., Bendix, J., 2019. Grassland ecosystem services in a changing environment: the potential of hyperspectral monitoring. *Remote Sens. Environ.* 232, 111273. doi:<https://doi.org/10.1016/j.rse.2019.111273>.
- Palmer, M.W., Earls, P.G., Hoagland, B.W., White, P.S., Wohlgemuth, T., 2002. Quantitative tools for perfecting species lists. *Environmetrics* 13, 121–137. doi:<https://doi.org/10.1002/env.516>.
- Pebesma, E., 2018. Simple features for R: standardized support for spatial vector data. *R J.* 10, 439. doi:<https://doi.org/10.32614/RJ-2018-009>.
- Pebesma, E., Bivand, R., 2023. Spatial Data Science: With Applications in R, 1st ed. Chapman and Hall/CRC, New York. doi:<https://doi.org/10.1201/9780429459016>.
- Pokrovsky, O., Roujeau, J.-L., 2003. Land surface albedo retrieval via kernel-based BRDF modeling: I. Statistical inversion method and model comparison. *Remote Sens. Environ.* 84, 100–119. doi:[https://doi.org/10.1016/S0034-4257\(02\)00100-1](https://doi.org/10.1016/S0034-4257(02)00100-1).
- Richter, R., Schläpfer, D., 2019. Atmospheric and topographic correction (ATCOR theoretical background document). DLR IB 1, 0564–03.
- Rossi, C., Kneubühler, M., Schütz, M., Schaepman, M.E., Haller, R.M., Risch, A.C., 2022. Spatial resolution, spectral metrics and biomass are key aspects in estimating plant species richness from spectral diversity in species-rich grasslands. *Remote Sens. Ecol. Conserv.* 8, 297–314. doi:<https://doi.org/10.1002/rse2.244>.
- Rüfenacht, D., Fredembach, C., Süsstrunk, S., 2014. Automatic and accurate shadow detection using near-infrared information. *IEEE Trans. Pattern Anal. Mach. Intell.* 36, 1672–1678. doi:<https://doi.org/10.1109/TPAMI.2013.229>.
- Schmidlein, S., Fassnacht, F., 2017. The spectral variability hypothesis does not hold across landscapes. *Remote Sens. Environ.* 192, 114–125. doi:<https://doi.org/10.1016/j.rse.2017.01.036>.
- Schweiger, A.K., Laliberté, E., 2022. Plant beta-diversity across biomes captured by imaging spectroscopy. *Nat. Commun.* 13, 2767. doi:<https://doi.org/10.1038/s41467-022-30369-6>.
- Serbin, S.P., Townsend, P.A., 2020. Scaling functional traits from leaves to canopies. In: Cavender-Bares, J., Gamon, J.A., Townsend, P.A. (Eds.), *Remote Sensing of Plant Biodiversity*. Springer International Publishing, Cham, pp. 43–82. doi:https://doi.org/10.1007/978-3-030-33157-3_3.
- Soffer, R.J., Gabriela, Ifimov, Arroyo-Mora, Juan Pablo, Kalacska, M., 2019. Validation of airborne hyperspectral imagery from laboratory panel characterization to image quality assessment: implications for an Arctic peatland surrogate simulation site. *Can. J. Remote. Sens.* 45, 476–508. doi:<https://doi.org/10.1080/07038992.2019.1650334>.
- St-Jean, S., Laliberté, E., 2020. Small Drone Photos - Open Vegetation Protocol.
- St-Jean, S., Vellend, M., 2020. Open Vegetation Survey Protocol.
- Thornley, R.H., Gerard, F.F., White, K., Verhoef, A., 2023. Prediction of grassland biodiversity using measures of spectral variance: a Meta-analytical review. *Remote Sens.* 15, 668. doi:<https://doi.org/10.3390/rs15030668>.
- Torresani, M., Rossi, C., Perrone, M., Hauser, L.T., Féret, J.-B., Moudry, V., Simova, P., Ricotta, C., Foody, G.M., Kacic, P., Feilhauer, H., Malavasi, M., Tognetti, R., Rocchini, D., 2024. Reviewing the spectral variation hypothesis: twenty years in the tumultuous sea of biodiversity estimation by remote sensing. *Ecol. Inform.* 102702. doi:<https://doi.org/10.1016/j.ecoinf.2024.102702>.
- Wallis, C.I.B., Crofts, A.L., Inamdar, D., Arroyo-Mora, J.P., Kalacska, M., Laliberté, É., Vellend, M., 2023. Remotely sensed carbon content: the role of tree composition and tree diversity. *Remote Sens. Environ.* 284, 113333. doi:<https://doi.org/10.1016/j.rse.2022.113333>.
- Wallis, C.I.B., Crofts, A.L., Inamdar, D., Arroyo-Mora, J.P., Kalacska, M., Laliberté, É., Vellend, M., 2024. Exploring the spectral variation hypothesis for α - and β -diversity: a comparison of open vegetation and forests. *Environ. Res. Lett.* doi:<https://doi.org/10.1088/1748-9326/ad44b1>.
- Wang, R., Gamon, J., 2019. Remote sensing of terrestrial plant biodiversity. *Remote Sens. Environ.* 231. doi:<https://doi.org/10.1016/j.rse.2019.111218>.
- Wang, R., Gamon, J.A., Cavender-Bares, J., Townsend, P.A., Zygielbaum, A.I., 2018. The spatial sensitivity of the spectral diversity–biodiversity relationship: an experimental test in a prairie grassland. *Ecol. Appl.* 28, 541–556. doi:<https://doi.org/10.1002/eap.1669>.

- Wang, R., Gamon, J.A., Cavender-Bares, J., 2022. Seasonal patterns of spectral diversity at leaf and canopy scales in the Cedar Creek prairie biodiversity experiment. *Remote Sens. Environ.* 280, 113169. <https://doi.org/10.1016/j.rse.2022.113169>.
- White, J.C., Coops, N.C., Wulder, M.A., Vastaranta, M., Hikler, T., Tompalski, P., 2016. Remote sensing Technologies for Enhancing Forest Inventories: a review. *Can. J. Remote. Sens.* 42, 619–641. <https://doi.org/10.1080/07038992.2016.1207484>.
- Zhang, L., Sun, X., Wu, T., Zhang, H., 2015. An analysis of shadow effects on spectral vegetation indexes using a ground-based imaging spectrometer. *IEEE Geosci. Remote Sens. Lett.* 12, 2188–2192. <https://doi.org/10.1109/LGRS.2015.2450218>.
- Zhang, C., Wang, Q., Atkinson, P.M., 2025. Unsupervised object-based spectral unmixing for subpixel mapping. *Remote Sens. Environ.* 318, 114514. <https://doi.org/10.1016/j.rse.2024.114514>.